Dr = transverse base dimension of a rib, in.
f_B = Blasius friction factor, $2 \cdot \Delta p \cdot g_c \cdot De/\rho \cdot u^2 \cdot Dl$, dimensionless
F = rib frequency or distance between corresponding points of successive ribs, in.
g_c = gravitational constant, 32.2 ft.lb.$_m$/lb.$_f$ sq. sec.
H = height of a rib or internal geometry, in.
K = coefficient in empirical correlation, $\Delta p = K \cdot u^\epsilon$
n = exponent in experimental correlation, $\Delta p = a \cdot u^n$
n_1 = number of ribs in a transverse row succeeding n_2
n_2 = number of ribs in a transverse row succeeding n_1
N = exponent in experimental correlation, $N_{Eu} = A \cdot N_{Re}^{-N}$
N_{Eu} = Euler number, $\Delta p \cdot g_c/\rho \cdot u^2$, dimensionless
N_{Re} = Reynolds number, $De \cdot u \cdot \rho/\mu$, dimensionless
Δp = pressure drop, lb./sq.in.
P = lineal perimeter of a noncorrugated rib, in.
Pc = lineal perimeter of a corrugated rib, in.
S = average plate spacing for fluid flow, in.
u = lineal fluid velocity in channel, ft./sec.
Wc = transverse width of plate channel between gaskets, in.
Y = plate separation or compressed gasket thickness, in.

Greek Letters

α = transverse rib angle for cross diagonal ribs, $\alpha = \theta$, radians
β' = exponent correlation for rib base angle effects
β = base angle of ribs, radians
B = coefficient correlation for rib base angle effects
γ = exponent correlation for rib corrugation effects
Γ = coefficient correlation for rib corrugation effects
δ = exponent correlation for plate separation effects
Δ = coefficient correlation for plate separation effects
ϵ = exponent in empirical correlation, $\Delta p = K \cdot u^\epsilon$
θ = transverse rib angle for diagonal ribs, radians
λ = exponent correlation for rib frequency effects
Λ = coefficient correlation for rib frequency effects
ρ = density of fluid, lb./cu.ft.
σ = exponent correlation for rib shape effects
Σ = coefficient correlation for rib shape effects
τ = exponent correlation for transverse rib angle efects
T = coefficient correlation for transverse rib angle effects
ϕ = exponent correlation for protrusions
Φ = coefficient for protrustions
ψ = rib shape geometrical parameter, $A_X/A_T - 1.0$, dimensionless

LITERATURE CITED

1. Troupe, R. A., J. C. Morgan, and J. Prifti, *Chem. Eng. Progr.*, **56**, No. 1, 124 (1960).
2. Seligman, R. J. S. and G. A. Dummett, *Chem. Ind,*. No. 38, 1602 (1964).
3. Baranovskii, N. V., "Plate-Type Heat Exchangers," pp. 122 to 148, Moscow, U.S.S.R. (1962).
4. Watson, E. L., A. A. McKillop, and W. L. Dunkly, *Ind. Eng. Chem.*, **52**, No. 9, 733-40 (1960).
5. Smith, V. C., and R. A. Troupe, *AIChE J.*, **11**, 487 (1965).
6. Maslov, A., *Molochnaya Promyshlennost,* **24,** No. 6, 17 (1963).
7. ———, *Pishchevaya Tekhnologiya,* No. 5, 143 (1964).
8. Buonopane, R. A., Ph.D. thesis, Northeastern Univ., Boston, Mass. (1967).

Manuscript received January 12, 1968; revision received April 22, 1968; paper accepted April 24, 1968.

Part II. Heat Transfer

Heat transfer and pressure drop data were taken on commercial plate heat exchange equipment. Nusselt and Euler correlations were determined for each of the six commercial heat exchangers investigated. These correlations were combined to establish a single heat transfer-pressure drop relationship for any plate type of heat exchanger channel.

The results of this investigation were tested by using the correlations developed in Part I of this series to predict pressure drop data for the commercial unit based on their channel geometries. These predicted pressure drops were then used with the results of this part of the series to predict and compare heat transfer data.

The correlations developed in this work allow one to determine the heat transfer characteristics in a ribbed rectangular channel from the pressure drop characteristics of the channel in question.

The effects of internal geometries on the pressure drop in ribbed rectangular channels have been correlated as functions of the rib and channel geometry in Part I of this series. Although the heat transfer characteristics of such channels are governed by the flow conditions, no attempts to correlate the heat transfer with pressure drop characteristics appear in the literature. Combined correlations relating heat transfer and pressure drop conditions have been determined for other types of turbulence producing channels (*1, 2*). This paper presents results which, when combined with those reported in Part I, will enable one to predict heat transfer characteristics from pressure drop conditions based on the rib and channel geometry.

In an investigation of flow in annuli containing finned turbulence promoters on the outer surface of the inner tube, Knudsen and Katz (*1*) obtained an empirical correlation containing dimensionless ratios of the fin height and spacing to the equivalent diameter of the channel. Sams (*2*), in an investigation of air flowing in ½ in. circular tubes with square-thread roughness elements on the inner surface, developed a friction factor correlation containing dimensionless ratios of the thread spacing and height to the thread width. He incorporated this friction factor into the Reynolds number group of an empirical Nusselt correlation thus combining the heat transfer and pressure drop correlations.

Extensive heat transfer studies have been conducted on plate and frame equipment (*3, 5* to *9*) all of which present results in the form of Nusselt correlations applicable to each individual exchanger investigated. The most complete presentation of Nusselt and Euler correlations for plate heat exchangers appears in Baranovskii's work (*3*). In all of the works cited above, the empirical Nusselt correlations are used only for the thermal design characteristics of the heat exchanger in question. Both Baranovskii (*4*) and Kovalenko (*10*) derive the correlation

$$\frac{\zeta}{2} \cdot \frac{u^2}{2 \cdot g_c \cdot Hp} \cdot \frac{Y}{Dl} \cdot \frac{t_2 - t_1}{\Delta t_{lm}} \cdot \frac{Cp \cdot \rho \cdot u}{U_{\text{avg.}}} = 1 \qquad (1)$$

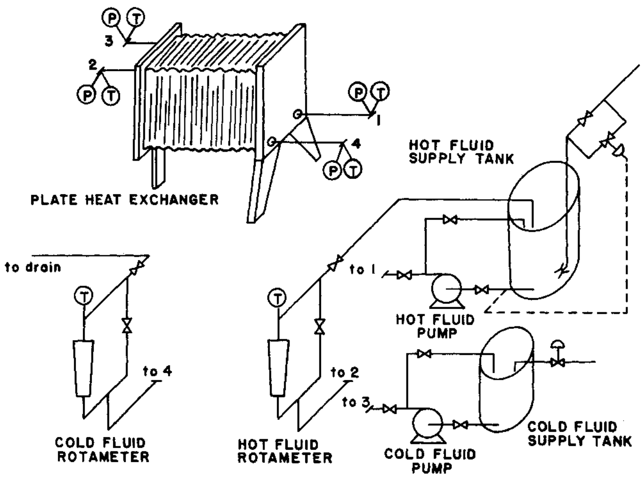

Fig. 1. Heat transfer study flow diagram.

for the combined thermal and hydraulic design of plate heat exchangers. Equation (1) may be simplified to the form:

$$N_{Eu} \cdot N_{Fr} \cdot \Gamma \cdot S' \cdot \frac{N_{Pe}}{N_{Nu}} = 1 \qquad (2)$$

Use of Equation (1) requires rearrangement to the form:

$$u = \sqrt[3]{\frac{U_{\text{avg.}} \cdot t_{lm} \cdot Dl \cdot g_c \cdot Hp}{\rho \cdot Cp \cdot (t_2 - t_1) \cdot Y \cdot \zeta}}$$

In this form an iteration procedure to determine corresponding thermal and hydraulic conditions is used as follows: (a) assume a linear velocity, u; (b) calculate the Euler number, $\zeta/2$, and the overall coefficient of heat transfer, $U_{\text{avg.}}$, from empirical correlations using the assumed linear velocity; (c) calculate the linear velocity from Equation (3); and (d) iterate until the assumed and calculated linear velocity agree. This iteration procedure is repeated for both fluids and provides the information needed to determine a looped flow streaming arrangement.

In an earlier investigation of plate heat exchangers, Böhm (*11*) determined an empirical Nusselt correlation involving a dimensionless parameter of the channel geometry but concluded that the channel geometry has a more significant effect on pressure drop than on heat transfer. The effects of rib and channel geometry on the pressure drop characteristics have been presented in Part I of this series. In the work presented here experimental studies were conducted to determine the heat transfer and pressure drop characteristics of six plate heat exchanger channels.

EXPERIMENTAL APPARATUS AND PROCEDURE

The arrangement of apparatus for the experimental investigation is shown in Figure 1. A 55 gal. drum was used to supply cold water to the system and a 90 gal. stainless steel tank was used to supply hot water. The hot water was heated to a controlled temperature by sparging with live steam. The cold water was taken at its ambient temperature from the main water supply. The hot and cold water flow rates were both metered by calibrated rotameters after passage through the heat exchanger being investigated. Both rotameters were connected with fully open or fully closed by-pass lines to extend their range to 30.3 gal./min. (hot fluid) and 37.7 gal./min. (cold fluid). Temperature measurements were made by means of copper sheathed iron-constantan thermocouples located in the entrance and exit ports of the heat exchanger. Each temperature was recorded (± 0.5°F.) on a 24 point, 0 to 300°F., temperature recorder every 18 sec. during a run. The pressure across the heat exchanger channels were measured by means of Bourdon type gauges connected to the entrance and exit ports of the heat exchanger.

In this work six different commercial plate heat exchangers were experimentally investigated. Data for a seventh heat exchanger was taken from work previously done by other investigators (*6, 12*). The characteristic dimensions of these plates are presented in Table 1. The experimental investigation for each exchanger consisted of varying the flow rates in both channels over the maximum range with the hot water inlet temperature held at three different levels between 125 and 200°F. Two different flow arrangements, Figure 2, were used. The actual flow rate range for each fluid and the hot water inlet temperature levels varied according to the duties of the particular exchanger being investigated.

TABLE 1. PLATE CHARACTERISTICS

	PLATE TYPE						
	A	B	C	D	E	F	G
Channel width between gaskets, ft.	0.7083	0.7813	0.5833	0.6667	0.6667	0.7708	0.9792
Compressed gasket spacing, ft.	0.0105	0.0196	0.0146	0.0142	0.0134	0.0114	0.0194
Plate thickness, ft.	0.0016	0.0033	0.0033	0.0029	0.0033	0.0029	0.0036
Heat transfer area per plate, sq. ft.	1.30	1.50	1.53	1.60	1.81	2.00	3.00

The following key will be used throughout this work to distinguish between the various plate types:

A = Triangular herringbone pattern.
B = Semicylindrical herringbone pattern.

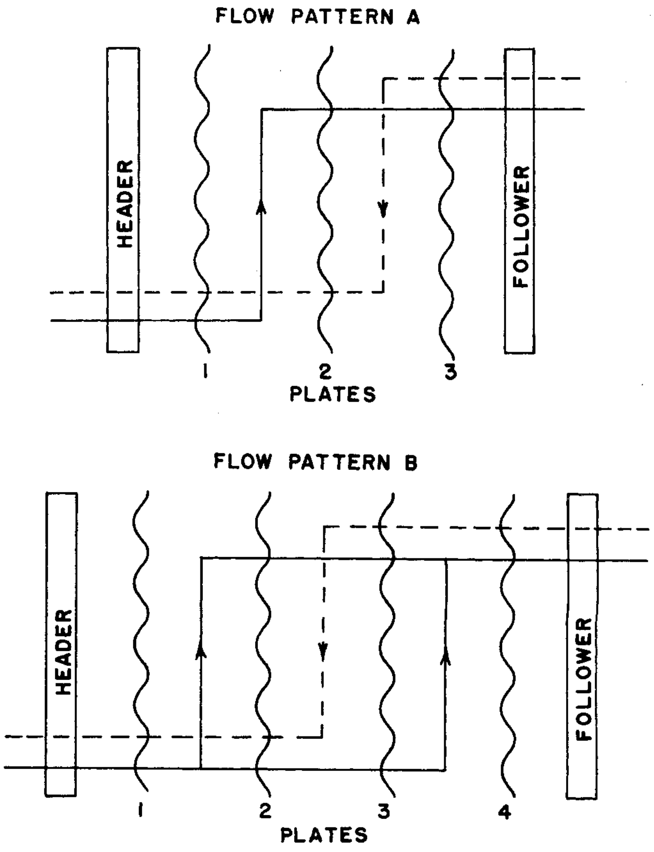

Fig. 2. Basic flow arrangements investigated.

C = Transverse trapezoidal pattern.
D = Semicylindrical diagonal crossed rib pattern.
E = Corrugated transverse triangular pattern.
F = Transverse triangular pattern.
G = Protrusions and depressions.

EVALUATION OF NUSSELT CORRELATIONS

The heat transfer data for each exchanger investigated was correlated in the form of the Nusselt equation:

$$N_{Nu} = C \cdot N_{Re}^{b} \cdot N_{Pr}^{0.4} \tag{4}$$

Because the flow channels for the fluid being heated and the fluid being cooled have the same geometric characteristics, the same Nusselt correlation is valid for both streams. The value of the Prandtl number exponent was taken as 0.4 in accordance with previous works (*3, 13* to *15*).

Rearranging the Nusselt correlation presented as Equation (4), one obtains the expression

$$\frac{C}{h} = \frac{De}{k} \cdot N_{Re}^{-b} \cdot N_{Pr}^{-0.4} \tag{5}$$

which may be evaluated for, C/h, at any value of b from experimental heat transfer data. Assuming negligible fouling and the same heat transfer area for both fluids, the resistance relationship for the overall heat transfer coefficient is:

$$\frac{1}{U_{\text{avg.}}} = \frac{1}{h_c} + \frac{x_p}{k_p} + \frac{1}{h_h} \tag{6}$$

The average overall heat transfer coefficient was calculated from experimental data from the expression:

$$U_{\text{avg.}} = \frac{Q_{\text{avg.}}}{A_p \cdot \Delta t_{lm}} \tag{7}$$

Because of the simple countercurrent flow arrangements used, no LMTD correction factor was required with Equation (7) in this work (*16, 17*).

The following iterative procedure was used to determine the values of the coefficient, C, and the Reynolds number exponent, b, which best fitted the experimental data for each exchanger investigated. A relationship for evaluating the Nusselt coefficient, C, for any value of the Reynolds number exponent, b, was obtained by rearranging the resistance relationship, Equation (6), to the form:

$$C = \frac{\dfrac{C}{h_c} + \dfrac{C}{h_h}}{\dfrac{1}{U_{\text{avg.}}} - \dfrac{x_p}{k_p}} \tag{8}$$

Values of the coefficient, C, were evaluated from Equation (8) for each exchanger investigated by: (a) assuming a value of the Reynolds number exponent, b; (b) calculating values of C/h_c and C/h_h for each experimental data point from Equation (5); and (c) calculating the average overall heat transfer coefficient for each experimental data point from Equation (7). Values for the coefficient, C, were determined at several values of the Reynolds number exponent, b, for each exchanger investigated. These values were then used to calculate an average overall coefficient of heat transfer from Equations (5) and (6). The final combination of the coefficient, C, and exponent, b, was taken as that which gave the minimum deviation when comparing the calculated [Equation (6)] and experimental [Equation (7)] average overall heat transfer coefficients. The values of C and b which best fitted the experimental data for each plate heat exchanger investigated are presented in Table 2. The average deviations between the calculated and experimental overall heat transfer coefficients using the values of C and b presented in Table 2 ranged from a maximum of ±8.8% to a minimum of ±2.6% with an average deviation of ±4.9% for the six commercial exchangers investigated.

A more detailed analysis of the Nusselt equation coefficient and the deviations of the experimental and calculated overall heat transfer coefficients was conducted (*18*) to determine the effects of fluid temperatures, fluid flow rates, and flow arrangements for each exchanger. Results of statistical analysis of variance calculations on the interaction of these effects on the coefficient, C, showed no dependency over the ranges investigated.

TABLE 2. EXPERIMENTAL NUSSELT CORRELATIONS
$N_{Nu} = C \cdot N^{b}_{Re} \cdot N^{0.4}_{Pr}$

Plate Type	C	b	Avg. Percent Deviation*
A	0.4322	0.62	±3.8
B	0.1431	0.79	±3.5
C	0.2536	0.65	†
D	0.3116	0.59	±7.3
E	0.1333	0.73	±2.6
F	0.2213	0.65	±3.2
G	0.1446	0.67	±8.8

* Deviation of $U_{\text{avg.}}$ calculated with C and b above from experimental $U_{\text{avg.}}$ for water ($t_{\text{avg.}}$ = 50 to 200°F., N_{Re} = 3,000 to 50,000)

$$\%\ \text{Dev.} = \frac{U_{\text{exp}} - U_{\text{calc}}}{U_{\text{exp}}} \times 100$$

† Data from (6).

EVALUATION OF EULER CORRELATIONS

Pressure drop data for each commercial exchanger investigated was directly correlated in the form

$$N_{Eu} = A \cdot N_{Re}^{-N} \tag{9}$$

The values of A and N calculated from a least-squares fit of all the data above a Reynolds number of 3,000 for each exchanger are presented in Table 3. These Euler correlations for the commercial plate heat exchangers are based on the overall pressure drop of the channel which includes the entrance and exit pressure drops as well as that of the ribbed plate section. The average deviations between the experimental and calculated Euler numbers using the values of A and N presented in Table 3 ranged from a maximum of ±73.4% to a minimum of ±31.0% with an average deviation of ±44.4% for the six commercial exchangers investigated. The accuracy of the pressure drop correlations were limited by the use of Bourdon pressure gauges and by operation of the commercial units to cover as wide a range of conditions as possible. It should be noted that unequal flow rates existing in adjacent flow streams cause plate buckling which changes the channel flow area and thus produces a wide variation in the pressure drop at any given flow rate.

CORRELATION OF HEAT TRANSFER AND PRESSURE DROP

Although the Nusselt and Euler correlations already evaluated are useful for a particular exchanger, they do not provide a true correlation between heat transfer and pressure drop useful for any heat exchanger with ribbed channels. A correlation between the film heat transfer coefficient and the pressure drop per unit heat transfer area for specified fluid properties was obtained from the results

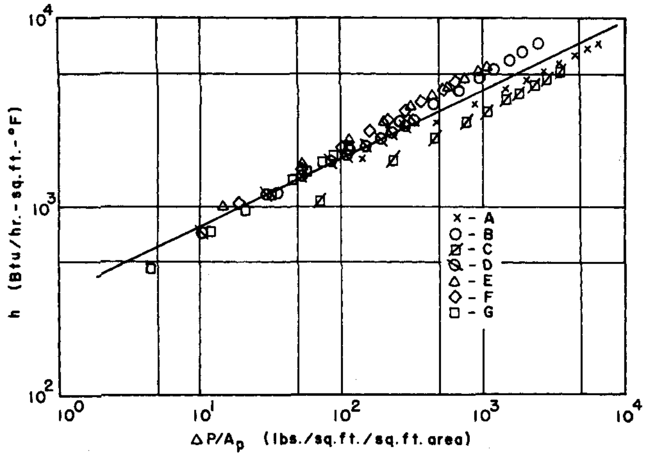

Fig. 3. Heat transfer-pressure drop correlation. (data for water at $t_{avg.} = 140°F.$)

presented here. This correlation, when combined with the results presented in Part I of this series, enables one to determine both the heat transfer and pressure drop characteristics from the rib and channel geometry.

Based on the fluid properties of water at 140°F., film heat transfer coefficients were evaluated from the Nusselt correlations presented in Table 2 and pressure drops were evaluated from the Euler correlations presented in Table 3. The film heat transfer coefficients were then plotted against the pressure drops per unit heat transfer area evaluated at ten Reynolds numbers between 3,000 and 30,000 for each plate heat exchanger. These results are shown in Figure 3.

A least-squares fit of the seventy data points used in Figure 3 provides the relation:

$$h = 360.7 \left(\frac{\Delta P}{Ap}\right)^{0.3544} \tag{10}$$

This expression is valid for the specific fluid properties of water at an average or bulk temperature of 140°F. and provides an average deviation of ±13.9% from the experimental film coefficients for the seven exchangers considered.

In evaluating the film coefficient at other temperatures, it was found that the exponent, 0.3544, remained constant and the coefficient changed by only ±14% over the temperature range from 80 to 200°F. Figure 4 shows the change in the coefficient of Equation (10) with changes in average fluid temperatures from 80 to 200°F. Film coefficients for fluids with properties similar to water at average or bulk temperatures other than 140°F. may be evaluated by using Equation (10) with the appropriate coefficient determined from Figure 4.

Table 3. Experimental Euler Correlations

$N_{Eu} = A \cdot N_{Re}^{-N}$

Plate Type	A	N	Avg. Percent Deviation*
A	2184.5	0.3178	73.4
B	715.7	0.1696	31.8
C	1543	0.306	†
D	1831.8	0.5116	45.1
E	86.4	0.0920	31.0
F	1573.9	0.4514	36.2
G	4875.8	0.5839	48.6

* Deviation of N_{Eu} calculated with A and N above from experimental N_{Eu} for water ($t_{avg.}$ = 50 to 200°F., N_{Re} = 3,000 to 50,000)

$$\% \text{ Dev.} = \frac{N_{Eu_{calc}} - N_{Eu_{exp}}}{N_{Eu_{exp}}} \times 100$$

† Data from (*12*).

APPLICATION OF RESULTS

The results of this investigation were combined with those presented in Part I of this series to test the possibility of predicting the heat transfer characteristics of the seven plate heat exchangers investigated. The ribbed section pressure drops were predicted from the rib and channel geometries using the correlations presented in Part I. Based on experimental results (*18*) for the particular entrance and exit shape used in Part I, the overall pressure drop was obtained by including 20% of the ribbed section pressure drop for entrance and exit losses for all plate types except G. For plate type G, entrance and exit losses equal to the ribbed section pressure drop were found to be experimentally accurate for this rib shape only (*18*). These overall pressure drops were then used with Equation (10) to predict film heat transfer coefficients for water at 140°F. with Reynolds numbers ranging from 3,000 to 30,000. Experimental film heat transfer coefficients were evaluated from the Nusselt correlations presented in Table 2. The average deviations of the film coefficients calculated using Equation (10) from the experimental values are presented in Table 4 for each of the seven commercial heat exchangers.

Table 4. Deviations of Film Coefficients Using Equation 10 at 140°F.

Plate Type	Percent Deviation from Experimental
A	+17.2
B	−37.2
C	−18.9
D	−9.6
E	−33.6
F	−9.0
G	−19.8

The results presented in Table 4 show that film coefficients of heat transfer were predicted with an average deviation of −15.8% from Euler correlations whose average deviations were ±44.4% and Nusselt correlations whose average deviations were ±4.9%. The improved accuracy of the heat transfer-pressure drop correlation [Equation (10)] is attributed to the fact that virtually no heat transfer takes place in the entrance and exit sections of plate heat exchanger channels. The overall pressure drop correlations presented in this work could undoubtedly be improved if a more detailed study of en-

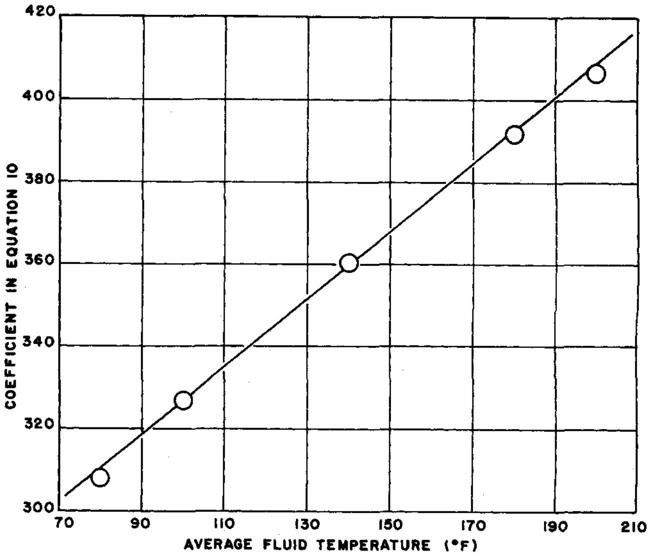

Fig. 4. Variation of coefficient in Equation (10) with temperature.

trance and exit pressure losses were conducted to replace the average value of 20% of the ribbed section pressure drop used here. Although this would improve the accuracy of the pressure drop correlations, it would not substantially increase the accuracy of predicting heat transfer data.

With the results presented in this paper and those presented in Part I of this series, one may determine Nusselt and Euler correlations for almost any type of ribbed channel. To accomplish this one should: (a) calculate a pressure drop-linear velocity correlation according to Part I of this series; (b) evaluate an Euler correlation using data obtained in step (a); (c) calculate film heat transfer coefficients from Equation (10); and (d) evaluate a Nusselt correlation from data obtained in step c. These Nusselt and Euler correlations may then be used to design heat transfer equipment using Equation (3) according to the methods of Baranovskii (*4*) or Kovalenko (*10*).

CONCLUSIONS

Based on the results reported in this work within the range of the variables investigated, it may be concluded that:

1. The heat transfer and pressure drop characteristics of ribbed channels similar to those investigated here may be predicted from the geometric characteristics of the channels.
2. The film coefficients of heat transfer in similar ribbed channels may be correlated with pressure drop according to the temperature dependent Equation (10).
3. The heat transfer conditions in plate heat exchanger channels operating with fluids similar to water may be predicted using the correlations presented here if one also includes an accurate estimate of the entrance and exit effects.
4. Although the results presented in this work cover a large range for plate heat exchanger operation, extrapolation and generalization beyond the range investigated is not recommended.

ACKNOWLEDGMENT

The authors gratefully acknowledge the cooperation of the Northeastern University Computation Center, the assistance of Richard E. King in collecting some of the experimental data, the fellowship support received from the Esso Foundation and N.D.E.A. for Dr. Ralph A. Buonopane, and a grant-in-aid received from Hercules Inc. for the purchase of accessory experimental equipment. The assistance of the following organizations is acknowledged for the use of their equipment: American Heat Reclaiming Corp., A.P.V. Co., Inc., Cherry-Burrell Corp., DeLaval Separator Corp., and Kusel Dairy Equipment Co.

NOTATION

- A = coefficient in experimental correlation, $N_{Eu} = A \cdot N_{Re}^{-N}$
- Ap = heat transfer surface area, sq.ft.
- b = exponent in experimental correlation, $N_{Nu} = C \cdot N_{Re}^{b} \cdot N_{Pr}^{0.4}$
- Cp = specific heat of fluid, B.t.u./lb.-°F.
- C = coefficient in experimental correlation, $N_{Nu} = C \cdot N_{Re}^{b} \cdot N_{Pr}^{0.4}$
- De = equivalent diameter of channel, ft.
- Dl = developed length of plate surface, ft.
- g_c = gravitational constant, 32.2 ft.-lb.$_m$/lb.$_f$-sq.sec.
- Hp = available fluid head, ft. of fluid
- h = film coefficient of heat transfer, B.t.u./hr.-sq.ft-°F.
- k = thermal conductivity, B.t.u./hr.-sq.ft.-°F./ft.
- N = exponent in experimental correlation, $N_{Eu} = A \cdot N_{Re}^{-N}$
- N_{Eu} = Euler number, $\Delta P \cdot g_c / \rho \cdot u^2$, dimensionless
- N_{Fr} = Froude number, $u^2 / 2 \cdot g_c \cdot Hp$, dimensionless
- N_{Nu} = Nusselt number, $h \cdot De/k$, dimensionless
- N_{Pe} = Peclet number, $N_{Re} \cdot N_{Pr}$, dimensionless
- N_{Pr} = Prandtl number, $Cp \cdot \mu / k$, dimensionless
- N_{Re} = Reynolds number, $De \cdot \rho \cdot u / \mu$, dimensionless
- ΔP = pressure drop in channel, lb./sq.ft.
- Q = hourly heat transfer rate, B.t.u./hr.
- S' = simplex of temperature conditions, $t_2 - t_1 / \Delta t_{lm}$, dimensionless
- t = temperature, °F.
- U = overall heat transfer coefficient, B.t.u./hr.-sq.ft.-°F.
- u = linear fluid velocity in channel, ft./sec.
- x = thickness of a heat transfer plate, ft.
- Y = plate separation or compressed gasket thickness, in.

Greek Letters

- Γ = simplex of geometry, Y/Dl, dimensionless
- ζ = frictional resistance coefficient, $2 \cdot N_{Eu}$, dimensionless
- μ = viscosity of fluid, lb./ft.-sec.
- ρ = density of fluid, lb./cu.ft.

Subscripts

- avg. = average or bulk fluid conditions
- c = cold fluid or fluid being heated
- calc = calculated or predicted value
- exp = experimental value
- h = hot fluid or fluid being cooled
- lm = logaritmic mean average
- p = characteristic of heat exchanger plate
- 1 = initial condition
- 2 = final condition

LITERATURE CITED

1. Knudsen, J. G., and D. L. Katz, *Chem. Engr. Progr.*, **46**, No. 10, 490 (1950).
2. Sams, E. W., *Natl. Advisory Comm. Aeronaut. Research Memo., E52D17* (1952).
3. Baranovskii, N. V., "Plate-Type Heat Exchangers," pp. 122 to 148, Moscow, U.S.S.R. (1962).
4. *Ibid.*, pp. 199 to 223.
5. McKillop, A. A., and W. L. Dunkley, *Ind. Eng. Chem.*, **52**, No. 9, 740 (1960).
6. Prifti, J. J., thesis, Northeastern Univ., Boston, Mass. (1959).
7. Ginstling, A. M., and V. V. Barsov, *Khimicheskoe Mashinostroenie*, No. 6, 20 (1959).
8. Barsov, V. V., *Khimicheskaya Promyshlennost*, No. 9, 663 (1962).
9. Jackson, B. W., and R. A. Troupe, *Chem. Engr. Progr.*, **60**, No. 7, 62 (1964).
10. Kovalenko, L. M., *Gidrolizn. i Lesokhim. Prom.*, No. 1, 17 (1964).
11. Böhm, *Kaltetechnik*, **7**, 358-62 (1955).
12. St. Ours, F. S., thesis, Northeastern Univ., Boston, Mass. (1964).
13. Antufev, K. M., and Yu. A. Lamm, *Tekhnch. inform. No. 8, Nevskogo mashinostreine zavoda im. V.I. Lenin, Mashgig* (1956).
14. Gebhardt, H., *Milchwissenschaft*, No. 7, 246 (1953).
15. Petukhov, B. S., *Gosznergoizdat* (1952).
16. Buonopane, R. A., R. A. Troupe, and J. C. Morgan, *Chem. Eng. Progr.*, **59**, No. 7, 57 (1963).
17. Jackson, B. W., and R. A. Troupe, *Chem. Engr. Progr. Symposium Ser., No. 64*, **62**, 185 (1966).
18. Buonopane, R. A., Ph.D. thesis, Northeastern Univ., Boston, Mass. (1967).

Manuscript received January 12, 1968; revision received April 22, 1968; paper accepted April 24, 1968.